

# Mechanism of proton- $^3\text{He}$ elastic backward scattering at intermediate energy

A.P. Kobushkin <sup>a,b</sup>, E.A. Strokovsky <sup>a,c</sup>, K. Hatanaka <sup>a</sup>,  
S. Ishikawa <sup>d</sup>

<sup>a</sup>*Research Center for Nuclear Physics, Osaka University, 10-1 Mihogaoka, Ibaraki  
Osaka, 567-0047, Japan*

<sup>b</sup>*Bogolyubov Institute for Theoretical Physics, Metrologicheskaya str. 14B, 03143  
Kiev, Ukraine*

<sup>c</sup>*LPP, Joint Institute for Nuclear Research, 141980, Dubna, Moscow region Russia*

<sup>d</sup>*Hosei University, Department of Physics, Fujimi 2-17-1, Chiyoda, Tokyo  
102-8160, Japan*

PACS number(s): 21.40.+d, 24.70.+5, 25.40.Cm, 25.55.Ci

---

## Abstract

We provide systematic analysis of the differential cross section of the proton- $^3\text{He}$  elastic scattering at  $\theta_{\text{cm}} = 180^\circ$ . It is shown that at energy from 0.2 to 1 GeV the mechanism, where momentum between the incoming and outgoing protons is transferred by rescattering of virtual pion on virtual deuteron, is the most important. Some predictions of this model for the differential cross section and the polarization correlation  $C_{yy}$  are discussed.

---

## 1 Introduction

For several decades considerable efforts have been done to investigate structure of the lightest nuclei (the deuteron,  $^3\text{He}$ ,  $^4\text{He}$ ) at short distances between the constituent nucleons. Significant progress was achieved both in theory and experiment, first of all because high quality data on spin-dependent observables were obtained with both hadronic [1,2] and electromagnetic probes [3]. Large part of these investigations consists of study of elastic backward (in the center of mass) proton – nucleus scattering (EBS). This process involves large momentum transfer  $|t|$  and therefore a belief exists that EBS can provide an access to the high momentum components of the wave function of the lightest nuclei.

The most detailed study of EBS was done for the deuteron where energy dependence of the differential cross section at  $\theta_{\text{cm}} = 180^\circ$ , the tensor analyzing power and the polarization transfer coefficient were measured (see [2] and Refs. therein). It became obvious that at present there is no theoretical model which quantitatively describe the existing data.

The elastic backward  $p(^3\text{He}, p)^3\text{He}$  scattering is studied in much less detail: only small amount of data points exist for the differential cross section at  $\theta_{\text{cm}} = 180^\circ$  and no data exist for spin-dependent observables. But presently, high intensity beams of polarized protons and polarized  $^3\text{He}$  targets offer an opportunity to perform as detailed studies of the elastic backward  $p(^3\text{He}, p)^3\text{He}$  scattering with spin dependent observables, as were already done for the deuteron case. On the other hand, this demands careful theoretical study of the  $p(^3\text{He}, p)^3\text{He}$  reaction mechanism. First of all it is necessary to find an adequate connection of this reaction with the structure of the  $3N$  system and get quantitative estimations for sensitivities of its cross section and spin-dependent observables to the existing wave functions of  $^3\text{He}$ .

The one-deuteron-exchange (ODE) of Fig. 1a shows that such connection exists. Still, it is obvious that at  $T_p > 200$  MeV this mechanism fails to reproduce detailed structure of existing data in both the nonrelativistic [4] and relativistic [5] approaches. Among other important mechanisms the so-called direct mechanism (DIR) of Fig. 1b may also play important role in this reaction, as it was pointed in Refs.[6,7].

Nevertheless ODE+DIR also cannot reproduce the “shoulder” in the measured energy dependence of the elastic differential cross section at  $\theta_{\text{cm}} = 180^\circ$  near  $T_p \sim 500$  MeV [8]. Note that similar situation takes place in the backward  $pd$  scattering<sup>1</sup>. Some authors try to connect this shoulder in the  $pd$  and  $p^3\text{He}$  scattering with pion exchange [7,10–14]. Fig. 1c demonstrates this mechanism for the case of  $p^3\text{He}$  scattering (later on it will be abbreviated as PI). PI includes  $pd \rightarrow \pi^3\text{He}$  as a subprocess, which has rather sharp resonance structure at energy kinematically close to the observed shoulder.

Calculations of the PI amplitude need care. Indeed the intermediate pion can be created by many ways, the most important of which are illustrated by diagrams of Fig. 1c1-c3. For example, it may come from the deuteron of  $^3\text{He}$  (see diagram (c1) of Fig. 1). It is clear that such pion exchange contributes to the  $^3\text{He}$  wave function and this diagram should be contained in the  $2N$  exchange. The diagram (c2) is already contained in DIR. So in our further calculations we take only diagram (c3) for the PI mechanism, where momentum between the incoming and outgoing protons is transferred by the backward pion elastic scattering on the intermediate deuteron. The differential cross section of this subprocess has a sharp resonance structure at energy near 200 MeV [15]. Similar mechanism for the backward  $pd$  scattering was discussed in [13,16].

---

<sup>1</sup> It was shown that one-neutron-exchange with the empirical momentum distribution of the nucleons in the deuteron extracted from  $A(d, p)X$  breakup describes the general behavior of the  $pd$  EBS cross section [9], but there is a small room for some additional contributions.

## 2 General formalism

Parity and time-reversal invariance leave only 8 independent complex amplitudes for the elastic scattering of two spin- $\frac{1}{2}$  particles. At  $\theta_{\text{cm}} = 180^\circ$  five of them vanish and they are reduced to

$$M(\theta_{\text{cm}} = 180^\circ) = \begin{pmatrix} M_{++}^{++} & M_{++}^{+-} & M_{-+}^{++} & M_{--}^{++} \\ M_{++}^{+-} & M_{++}^{--} & M_{-+}^{+-} & M_{--}^{+-} \\ M_{-+}^{++} & M_{-+}^{+-} & M_{-+}^{--} & M_{--}^{--} \\ M_{--}^{++} & M_{--}^{+-} & M_{-+}^{--} & M_{--}^{--} \end{pmatrix} = \begin{pmatrix} A & 0 & 0 & 0 \\ 0 & F & G & 0 \\ 0 & G & F & 0 \\ 0 & 0 & 0 & A \end{pmatrix} \quad (1)$$

Here  $M_{Mm}^{M'm'}$  is amplitude with  $M, m$  and  $M', m'$  magnetic quantum numbers of  ${}^3\text{He}$  and the proton in initial and final states, respectively. We assume the normalization when the differential cross section is given by

$$\frac{d\sigma}{d\Omega_{\text{cm}}} = \frac{\frac{1}{4}\text{Tr}(MM^\dagger)}{64\pi^2 s} = \frac{|A|^2 + |F|^2 + |G|^2}{128\pi s}, \quad (2)$$

where  $s$  is the total c.m. energy squared and the factor  $\frac{1}{4}$  comes from the average over initial spin states.

Corresponding to the three non-vanishing amplitudes there are  $2 \times 3 - 1 = 5$  independent observables: the differential cross section (2) and 4 spin-dependent observables. Among the last ones we will consider in this paper only polarization correlation

$$C_{yy} = \frac{\text{Tr}(M\sigma_y(\text{He})M^\dagger\sigma_y(p))}{\text{Tr}(MM^\dagger)} = \frac{2\text{Re}(AG^*)}{|A|^2 + |F|^2 + |G|^2}. \quad (3)$$

The ingredients necessary for calculation of the amplitudes  $A, F$  and  $G$  are considered in the next section.

## 3 Derivation of reaction amplitude

### 3.1 ${}^3\text{He}$ wave function

The virtual  ${}^3\text{He} \rightarrow d + p$  decay amplitude reads

$$\bar{u}_m(p)\Gamma_\mu\varepsilon^\mu(\sigma)U_M(P) = (2\pi)^{\frac{3}{2}}2\sqrt{m_\tau}(p^2 - m_p^2 + i0)\psi_M^{\sigma m}(\vec{k}). \quad (4)$$

Here and later on we use the following notations:  $m_p$ ,  $m_d$  and  $m_\tau$  are masses,  $p$ ,  $p_d$  and  $P$  are momenta and  $m$ ,  $\sigma$ ,  $M$  are magnetic quantum numbers of the proton, the deuteron and  ${}^3\text{He}$ , respectively;  $\vec{k} = \frac{2}{3}\vec{P} - \vec{p}_d$  is the relative momentum between the proton and the deuteron in  ${}^3\text{He}$ ;  $\varepsilon^\mu(\sigma)$  is the polarization vector of the deuteron,  $u_m(p)$  and  $U_M(P)$  are spinors for the proton and  ${}^3\text{He}$ ;  $\psi_M^{\sigma m}(\vec{k})$  is the overlap between the  ${}^3\text{He}$  and  $p + d$  wave functions, i.e. it is a wave function for the relative motion of the proton and the deuteron inside  ${}^3\text{He}$ . It has the following form

$$\psi_M^{\sigma m}(\vec{k}) = \left\{ \sqrt{\frac{1}{4\pi}} u(k) \left\langle 1 \frac{1}{2} \sigma m \left| \frac{1}{2} M \right. \right\rangle + w(k) \sum_{\xi, l_3} \langle 21l_3 \sigma | 1\xi \rangle \left\langle 1 \frac{1}{2} \xi m \left| \frac{1}{2} M \right. \right\rangle Y_{2l_3}(\hat{k}) \right\}. \quad (5)$$

The quantity

$$n_d(k) \equiv \frac{1}{2J_\tau + 1} \sum_{M, \sigma, m} \left| \psi_M^{\sigma m}(\vec{k}) \right|^2 = u^2(k) + w^2(k) \quad (6)$$

has meaning of the deuteron momentum distribution in  ${}^3\text{He}$  and  $N_d = \int d^3k n_d(k)$  is the effective number of deuterons in  ${}^3\text{He}$ .

### 3.2 ODE approximation

In the nonrelativistic limit and at  $\theta_{\text{cm}} = 180^\circ$  the corresponding amplitudes  $A^{\text{ODE}}$ ,  $F^{\text{ODE}}$  and  $G^{\text{ODE}}$  of (1) read

$$A^{\text{ODE}} = \frac{1}{3} t_0 \left[ u^2(k) - 2\sqrt{2}u(k)w(k) + \frac{2}{3}w^2(k) \right], \quad (7)$$

$$F^{\text{ODE}} = \frac{1}{3} t_0 \left[ 2u^2(k) + 2\sqrt{2}u(k)w(k) + w^2(k) \right], \quad (8)$$

$$G^{\text{ODE}} = \frac{1}{3} t_0 \left[ -u^2(k) + 2\sqrt{2}u(k)w(k) - 2w^2(k) \right], \quad (9)$$

$$t_0 = 4(2\pi)^3 m_\tau m_p \left( \varepsilon - \frac{\vec{k}^2}{2\mu_{pd}} \right), \quad (10)$$

where  $\mu_{pd} = \frac{m_p m_d}{m_p + m_d}$  and  $\varepsilon$  is the binding energy.

To take into account relativistic effects we use dynamics in infinite momentum frame (IMF). This can be done easily by repeating arguments of Ref.[9], which finally are reduced to the two prescriptions:

- substitute new argument in the wave functions  $u(k) \rightarrow u(k_{\text{IMF}})$ ,  $w(k) \rightarrow w(k_{\text{IMF}})$
- change the factor  $t_0 \rightarrow 2(2\pi)^3 \frac{\epsilon_p \epsilon_d (M_{dp}^2 - m_\tau^2)}{(\epsilon_p + \epsilon_d)(1-\alpha)}$

In these prescriptions the relativistic internal momentum,  $k_{\text{IMF}}$ , the invariant mass of virtual  $d+p$  pair,  $M_{dp}$ , and other variables are expressed in terms of the c.m. momentum and energies of colliding particles,  $p^*$ ,  $E_p^*$  and  $E_\tau^*$ , respectively, as follows:

$$k_{\text{IMF}} = \sqrt{\frac{\lambda(M_{dp}^2, m_d^2, m_p^2)}{4M_{dp}^2}}, \quad (11)$$

$$M_{dp}^2 = \frac{m_p^2}{\alpha} - \frac{m_d^2}{1-\alpha}, \quad \epsilon_p = \sqrt{m_p^2 + k_{\text{IMF}}^2}, \quad \epsilon_d = \sqrt{m_d^2 + k_{\text{IMF}}^2}, \quad (12)$$

where  $\alpha = \frac{E_p^* + p^*}{E_\tau^* + p^*}$  is the fraction of the incoming  ${}^3\text{He}$  momentum carried by the outgoing proton in IMF.

### 3.3 Direct mechanism in optimal approximation

Importance of DIR in the elastic backward proton-nucleus scattering was emphasized in [6], where an approximation which minimizes the binding energy and recoil corrections was derived. The approximate amplitudes of Fig. 1b are factorized into the  ${}^3\text{He}$  body form factor,  $F(q^2)$ , and the on-shell proton-proton amplitude at the effective energy,  $f_{pp}(E_{\text{eff}}, \theta)$ , where  $E_{\text{eff}}$  corresponds to such total energy in the Breit frame as if the struck proton takes all the momentum of  ${}^3\text{He}$  [6]. If one neglects spin structure of the  $pp$ -scattering (which seems to be a good approximation for the reaction at  $\theta_{\text{cm}} = 180^\circ$ ) the DIR amplitudes read:

$$A^{\text{DIR}} = F^{\text{DIR}} = 8\pi\sqrt{s}f_{pp}(E_{\text{eff}}, \theta)F(q^2), \quad G^{\text{DIR}} = 0. \quad (13)$$

The form factor is given by

$$F(q^2) = F_S(q^2) + F_D(q^2), \quad (14)$$

$$F_S(q^2) = \int_0^\infty dr j_0\left(\frac{2}{3}qr\right)u^2(r), \quad F_D(q^2) = \int_0^\infty dr j_0\left(\frac{2}{3}qr\right)w^2(r). \quad (15)$$

In our calculations, because of the identity of the protons, we use the standard parameterization of the  $pp$  scattering amplitude  $f_{pp} = \frac{p^*}{4\pi}(i + \rho_{pp})\sigma_{pp}^{\text{tot}}e^{-\frac{1}{2}bu}$ , where  $\rho_{pp}$  is the ratio of the real to imaginary part of the scattering amplitude,  $\sigma_{pp}^{\text{tot}}$  is the total cross section and  $b$  is the slope parameter of the elastic  $pp$ -scattering.

### 3.4 High momentum transfer by intermediate pion

The matrix element corresponding to the diagram (c3) of Fig. 1 reads:

$$\begin{aligned}
\mathcal{M}_{mM}^{m'M'}(\text{PI}) = & \left(\frac{1}{2\pi}\right)^8 \left(2m_p \frac{f_{\pi NN}}{\mu}\right)^2 \int d^4 p_d d^4 p'_d \sum_{\sigma\sigma'} A_{\sigma\sigma'} F_\pi^2(q^2) \times \\
& \times \bar{u}_{m'}(p') \gamma_5 \frac{1}{\not{p}' - m_p + i0} \Gamma_\mu \varepsilon^\mu(\sigma') U_M(P) \times \\
& \times \overline{U}_{M'}(P') \Gamma^\nu \varepsilon_\nu^*(\sigma) \frac{1}{\not{p}' - m_p + i0} \gamma_5 u_m(p) \times \\
& \times \frac{1}{(p_d^2 - m_d^2 + i0)(p_d'^2 - m_d^2 + i0)(q^2 - \mu^2 + i0)(q'^2 - \mu^2 + i0)}, \tag{16}
\end{aligned}$$

where  $A_{\sigma\sigma'}$  is an amplitude of the subprocess  $\pi^0 d \rightarrow \pi^0 d$ ,  $\mu$  is the pion mass,  $F_\pi(q^2)$  and  $f_{\pi NN}$  are the form factor and coupling constant of the  $\pi NN$  vertex. The spinors are normalized as  $\bar{u}_m(p)u_{m'}(p) = \delta_{mm'}$ , etc. Integrating over the deuteron energies one gets

$$\begin{aligned}
\mathcal{M}_{mM}^{m'M'}(\text{PI}) = & - \left(\frac{1}{2\pi}\right)^6 \left(2m_p \frac{f_{\pi NN}}{\mu}\right)^2 4m_\tau (2\pi)^3 \int \frac{d^3 p_d}{2E_d} \frac{d^3 p'_d}{2E'_d} \sum_{\sigma\sigma'} A_{\sigma\sigma'} \times \\
& \times F_\pi^2(q^2) \chi_{m'}^\dagger \vec{Q}' \vec{\sigma} \chi_{\tilde{m}'} \chi_{\tilde{m}}^\dagger \vec{Q} \vec{\sigma} \chi_m \frac{\psi_{M'}^{*\sigma\tilde{m}}(\vec{k}) \psi_M^{\sigma'\tilde{m}'}(\vec{k}')}{(q^2 - \mu^2 + i0)(q'^2 - \mu^2 + i0)}, \tag{17}
\end{aligned}$$

where  $\chi_{m(m')}$  and  $\chi_{\tilde{m}(\tilde{m}'')}$  are Pauli spinors for the protons,  $\vec{Q} = \sqrt{\frac{E_p+m_p}{E_l+m_p}} \vec{l} - \sqrt{\frac{E_l+m_p}{E_p+m_p}} \vec{p}$ ,  $\vec{Q}' = \sqrt{\frac{E_{p'}+m_p}{E_{l'}+m_p}} \vec{l}' - \sqrt{\frac{E_{l'}+m_p}{E_{p'}+m_p}} \vec{p}'$  and  $E_d = \sqrt{\vec{p}_d^2 + m_d^2}$ ,  $E'_d = \sqrt{\vec{p}'_d^2 + m_d^2}$ .

To simplify loop integration we take out of the integral the amplitude  $A_{\sigma\sigma'}$  and the form factors  $F_\pi^2(q^2)$  at point where the deuteron carries  $\frac{2}{3}$  of the  ${}^3\text{He}$  momentum. To take into account Fermi motion of the deuteron in  ${}^3\text{He}$ , these factors were averaged over Gaussian distribution with  $\langle p_d^2 \rangle^{1/2} = 50$  MeV/c. The latter value was taken from the calculated deuteron momentum distribution in  ${}^3\text{He}$ . Finally one gets:

$$\begin{aligned}
\mathcal{M}_{mM}^{m'M'}(\text{PI}) = & - \left(\frac{1}{2\pi}\right)^3 \left(2m_p \frac{f_{\pi NN}}{\mu}\right)^2 4m_\tau \sum_{\sigma\sigma'} \langle A_{\sigma\sigma'} F_\pi^2 \rangle \times \\
& \times \chi_{m'}^\dagger \sigma_j \chi_{\tilde{m}'} \chi_{\tilde{m}}^\dagger \sigma_i \chi_m \mathcal{Q}_{jM'}^{\sigma\tilde{m}} \mathcal{Q}_{iM}^{\sigma'\tilde{m}'} \tag{18}
\end{aligned}$$

$$\mathcal{Q}_{jM'}^{\sigma\tilde{m}} = \int \frac{d^3 p_d Q_j \psi_{M'}^{*\sigma\tilde{m}}(\vec{k})}{2E_d(q^2 - \mu^2 + i0)}, \quad \mathcal{Q}_{iM}^{\sigma'\tilde{m}'} = \int \frac{d^3 p'_d Q'_i \psi_M^{\sigma'\tilde{m}'}(\vec{k}')}{2E'_d(q'^2 - \mu^2 + i0)}, \tag{19}$$

$$\langle A_{\sigma\sigma'} F_\pi^2 \rangle = \frac{2\pi}{\langle p_d^2 \rangle^{1/2}} \int_{-\infty}^{\infty} d\tilde{p} e^{-\frac{(\tilde{p}-p^*)^2}{\langle p_d^2 \rangle}} A_{\sigma\sigma'}(\tilde{s}_{\pi d}, 180^\circ) F_\pi^2(\tilde{q}^2). \quad (20)$$

Now there are two independent three-dimensional integrals and the integration over angles can be done analytically in the nonrelativistic limit.

#### 4 Numerical calculations, comparison with experiment and predictions

In the present calculations, the  $p + d$  relative wave functions inside  ${}^3\text{He}$ ,  $u(k)$  and  $w(k)$  in Eq.(6), are projected out from the  ${}^3\text{He}$  wave function obtained by the Faddeev calculation [17] with Argonne V18 potential [18]. These are parameterized by the sum of Gaussians,

$$u(k) = \sum_{i=1}^N A_i e^{-\alpha_i k^2}, \quad w(k) = k^2 \sum_{i=1}^N B_i e^{-\beta_i k^2}. \quad (21)$$

The parameters are summarized in Table 1. The standard parameterization of the form factor  $F_\pi(q^2) = (\Lambda^2 - \mu^2)/(\Lambda^2 - q^2)$  with  $\Lambda = 1300$  MeV and  $f_{\pi NN}^2/4\pi = 0.08$  [19] was used. Amplitudes  $A_{\sigma\sigma'}$  are taken from the partial wave analysis by Virginia group [20].

Results of the calculations are compared with experimental data for the differential cross section on Fig. 2. To demonstrate, up to which extent the reaction is sensitive to the potential model, we also provide calculations with the wave function with Urbana potential [24]. One sees that (qualitatively) Urbana potential gives similar result, but it is systematically higher (with factor 1.5-2.5) in comparison with the result with Argonne potential. It also overestimates the experimental data.

Predictions for the polarization correlation  $C_{yy}$  are displayed in Fig. 3.

Figs. 2 and 3 demonstrate that at  $T_p \approx 200$  MeV the cross section and the spin-dependent observables should have sharp structure which comes from the interference of two mechanisms, ODE and PI.

#### 5 Conclusions

The main results of this work can be summarized as follows:

- There are three kinematical regions where different mechanisms determine the proton- ${}^3\text{He}$  backward elastic scattering: up to  $T_p \sim 200$  MeV ODE dominates; between  $200 < T_p < 1000$  MeV the reaction is dominated by PI and at higher energies

the dominating mechanism is DIR. The same must be true also for other backward scattering reactions with the lightest nuclei at intermediate energy.

- The results obtained here give a qualitative confirmation that intermediate  $\pi d \rightarrow d\pi$  resonance scattering is responsible for the enhancement observed in the differential cross section at  $0.4 < T_p < 0.8$  GeV.
- All the mechanisms, ODE, DIR and PI, are deeply connected with the  $^3\text{He}$  structure. Elastic backward scattering of the proton on  $^3\text{He}$  can be used as a source of information about the  $^3\text{He}$  structure at short distances.
- The model predicts a structure in energy dependence of the differential cross section and spin-dependent observables near  $T_p \approx 200$  MeV, which comes from the interference between ODE and PI mechanisms.

All these predictions can be experimentally verified at RCNP.

The authors would like to thank M. Tanifuji and H. Toki for stimulating discussions. One of us (A.P.K.) is grateful to A. Boudard for sending the numerical cross section data obtained at SATURNE. Two of the authors (A.P.K., E.A.S.) acknowledge the hospitality of RCNP, where this work was carried out with a Center of Excellence grant from the Ministry of Education, Culture, Sports, Science and Technology (Monbu-Kagaku-sho), Japan.

## References

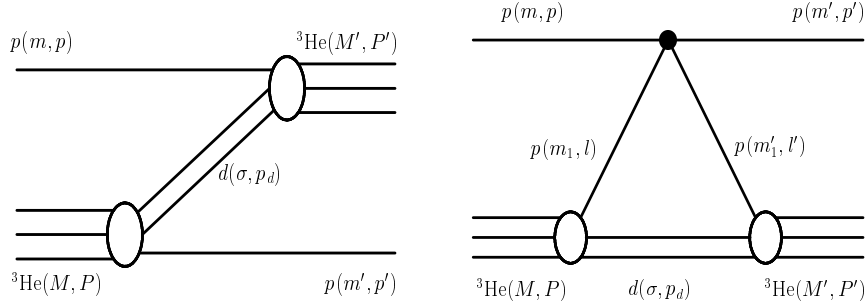
- [1] V.G. Ableev et al., Pis'ma ZhETF 37 (1983) 196 [JETP Lett. 37 (1983) 233]; Nucl. Phys. A393 (1983) 491, A411 541(E); Pis'ma ZhETF 45 (1987) 467 [JETP Lett. 45 (1987) 596]; JINR Rapid Comm. 1[52]-92 (1992) 10; Few Body Systems 8 (1990) 137; C.F. Perdrisat et al., Phys. Rew. Lett 59 (1987) 2840; V. Punjabi et al., Phys. Rev. C39 (1989) 608.
- [2] L.S. Azhgirey et al., Yad. Fiz. 61 (1998) 494 [Phys. At. Nucl. 61 (1998) 432]; V. Punjabi et al., Phys. Lett. B350 (1995) 178.
- [3] I. Sick, Progress in Particle and Nuclear Physics 47 (2001) 245; A.P. Kobushkin and Ya.D. Krivenko, nucl/th 0112009.
- [4] H. Leśniak and L. Leśniak, Acta Phys. Pol. B9 (1978) 419.
- [5] A.P. Kobushkin, In: Proc. Int. Conf. DEUTERON-93, ed. V.K. Lukyanov (Dubna, 14-18 Sept., 1993) p.71.
- [6] S.A. Gurvitz, J.-P. Dedonder and R.D. Amado, Phys. Rev. C19 (1979) 142; S.A. Gurvitz, Phys. Rev. C20 (1979) 1256.
- [7] Yu.N. Uzikov, Nucl. Phys. A644 (1998) 321.
- [8] R. Frascaria et al., Phys. Lett. 66B (1977) 329; P. Berthet et al., Phys. Lett. 106B (1981) 465.

- [9] A.P. Kobushkin, *J. Phys. G* 12 (1986) 487.
- [10] N.S. Cragie and C. Wilkin, *Nucl. Phys. B* 14 (1969) 477.
- [11] V.M. Kolybasov and N.Ya. Smorodinskaya, *Phys. Lett. B* 37 (1971) 272; *Yad. Fiz.* 17 (1973) 1211 [*Sov. J. Nucl. Phys.* 17 (1973) 630].
- [12] G.W. Barry, *Phys. Rev. D* 7 (1973) 1441.
- [13] L.A. Kondratyuk and F.M. Lev, *Yad. Fiz.* 26 (1977) 294 [*Sov. J. Nucl. Phys.* 26 (1977) 153].
- [14] A. Nakamura and L. Satta, *Nucl. Phys. A* 445 (1985) 706.
- [15] H. Garsilazo and T. Mitsutani,  $\pi NN$  Systems (World Scientific, Singapore, 1990).
- [16] J.C. Anjos, A. Santoro, F.R.A. Simao and D. Levy, *Nucl. Phys. A* 356 (1981) 383.
- [17] Y. Wu, S. Ishikawa, T. Sasakawa, *Few-Body Syst.* 15 (1993) 145.
- [18] R.B. Wiringa, V.G.J. Stokes, R. Schiavilla, *Phys. Rev. C* 51 (1995) 38.
- [19] R. Machleidt, K. Holinde and Ch. Elster, *Phys. Rep.* 149 (1981) 1.
- [20] R.A. Arndt, I.I. Strakovsky and R.L. Workman, *Phys. Rev. C* 50 (1994) 1796.
- [21] C.C. Kim et al., *Nucl. Phys.* 58, (1964) 32.
- [22] L.G. Votta et al., *Phys. Rev. C* 10 (1974) 520.
- [23] H. Langevin-Joliot et al., *Nucl. Phys. A* 158 (1970) 309.
- [24] R. Schiavilla, V.R. Pandharipande and R.B. Wiringa, *Nucl. Phys. A* 449 (1986) 219.

Table 1

Parameters of the  $^3\text{He}$  wave function with Argonne V18 potential parameterized by (21).

	$A_i$ GeV $^{-3/2}$	$\alpha_i$ GeV $^{-2}$	$B_i$ GeV $^{-7/2}$	$\beta_i$ GeV $^{-2}$
1	15.877531	298.42	38.675388	354.79
2	-13.052731	238.79	46.368992	117.91
3	10.436090	142.99	21.285334	45.409
4	4.0535767	57.857	5.3864329	19.864
5	1.9751837	28.251	.86501103	9.9491
6	.51022908	13.693	.10750704	5.3389
7	-.13970059	6.2369	.31609429E-1	1.8140
8	-.5010875E-1	3.2592	-.76611531E-1	1.4127
9	.1447265E-1	1.5734	.71395663E-3	.99982
10	-.1003085E-1	.78261	.45173853E-1	1.1447
11	.6741846E-2	.43514	-.17644911E-2	.39628
12	-.1115674E-2	.14656	-.71439194E-3	.17188



(a)

(b)

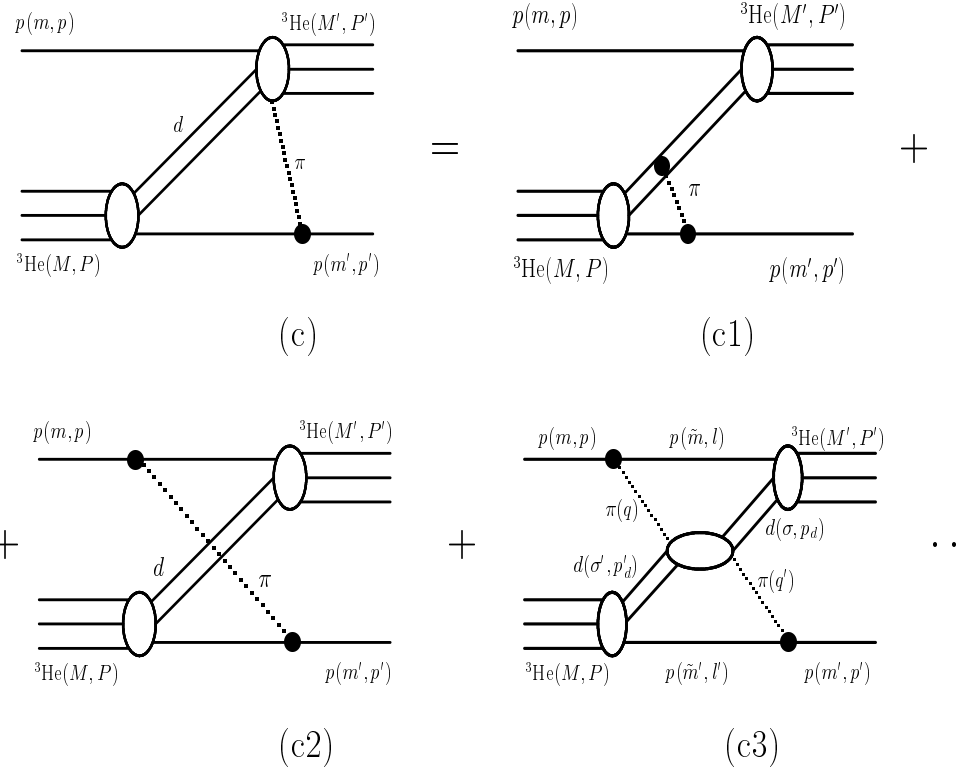


Fig. 1. Reaction mechanisms of the  $p^3\text{He}$  elastic backward scattering: one deuteron exchange (ODE, (a)), direct mechanism (DIR, (b)) and the “triangle” diagram, (c). The diagrams (c1), (c2) and (c3) are subprocesses contributing to the triangle diagram.

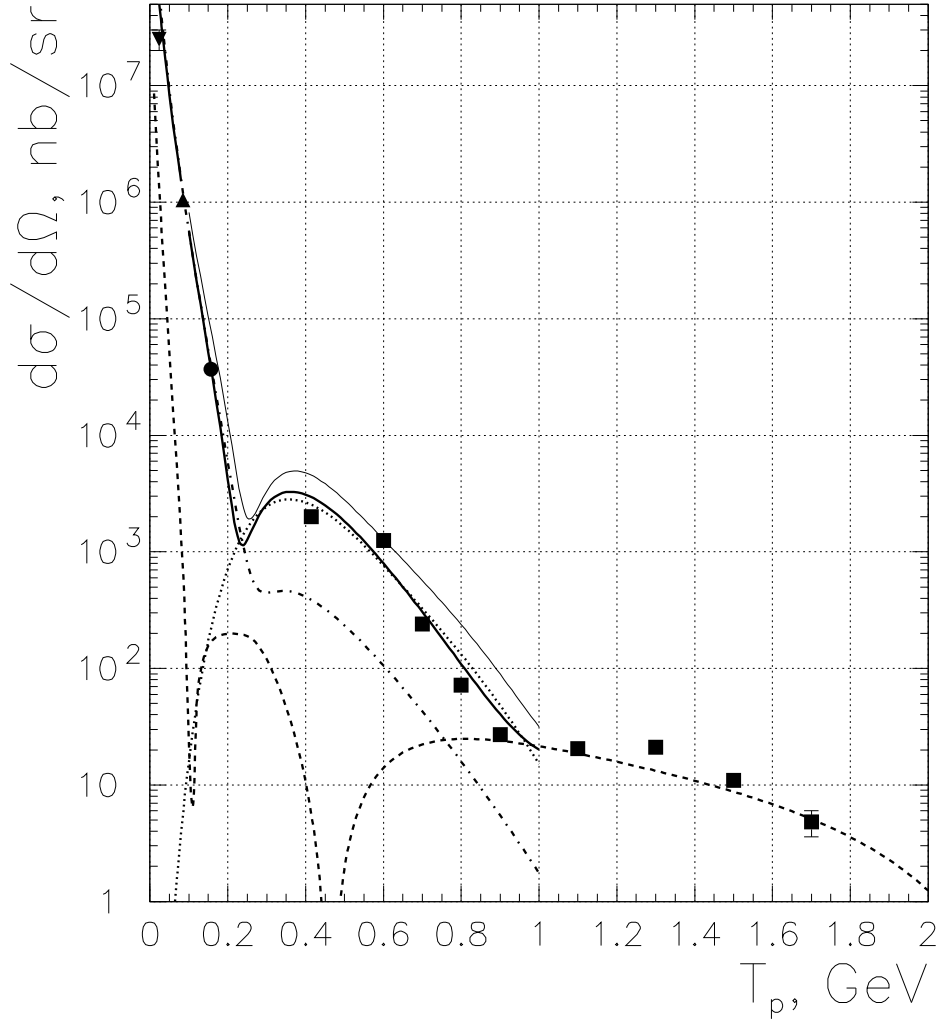


Fig. 2. Differential elastic cross section at  $\theta_{\text{cm}} = 180^\circ$ . The bold solid line represents ODE+DIR+PI for the wave function with Argonne V18 potential. The dot-dashed and dashed lines represent the ODE and DIR mechanisms, respectively. The dotted line is for the PI mechanism. The thin solid line represents ODE+DIR+PI for the wave function with Urbana potential. Data are from: square — [8], “down” triangle — [21], “up” triangle — [22] and circle — [23]. Data [21–23] were extrapolated to  $\theta_{\text{cm}} = 180^\circ$  by us.

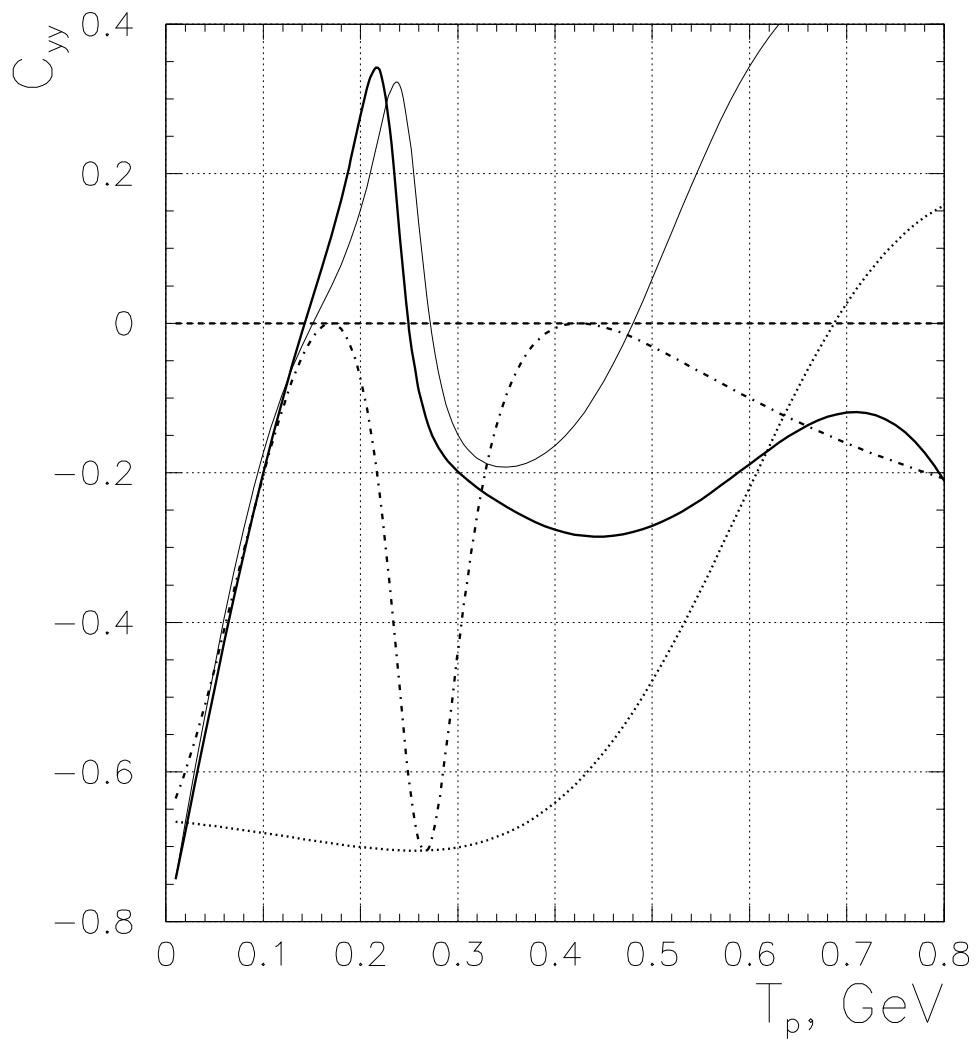


Fig. 3. Predictions of the model for the polarization correlation  $C_{yy}$ . The lines are the same as at Fig. 2.